Progress in theoretical understanding of the Dimits shift and the tertiary instability in drift-wave turbulence

Hongxuan Zhu[1] (hzhu@pppl.gov), Yao Zhou[1], and I. Y. Dodin[1,2]

[1] Princeton Plasma Physics Laboratory [2]Princeton University

Background

- The Dimits shift is the shift between the linear primary-instability threshold and the actual onset of turbulent transport seen in gyrokinetic simulations [1].
- Zonal flows (ZFs) are believed to suppress drift-wave (DW) turbulence within the Dimits shift. Such ZFs must be stable to the tertiary instability (TI) [2].
- The TI mode in electrostatic DW turbulence tend localize near the extrema of the ZF velocity $U(x)$, as seen in many simulations using different models [2, 3, 4].

Motivation: localized TI modes in the mHWE (resistive electrostatic DW turbulence)

- The mHWE describes 2D DW turbulence immersed in a uniform magnetic field along z:

$$(\partial_t + \hat{\boldsymbol{z}} \times \nabla\varphi \cdot \nabla) w = \kappa \partial_y \varphi - \hat{D} w, \quad (\partial_t + \hat{\boldsymbol{z}} \times \nabla\varphi \cdot \nabla) n = \alpha(\tilde{\varphi} - \tilde{n}) - \kappa \partial_y \varphi - \hat{D} n. \tag{1}$$

  Here, $\nabla = (\partial_x, \partial_y)$, φ is the electrostatic potential fluctuation, n is the density fluctuation, $w \doteq \nabla^2\varphi - n$, κ models density gradient, α is the "adiabaticity parameter".
- Denote $\langle \dots \rangle$ as the zonal average (average in y). The zonal average of Eqs. (1) are

$$\partial_t U = -\partial_x \langle \tilde{v}_x \tilde{v}_y \rangle - \hat{D} U, \quad \partial_t N = -\partial_x \langle \tilde{v}_x \tilde{n} \rangle - \hat{D} N, \tag{2}$$

  where $U(x,t) \doteq \partial_x \langle \varphi \rangle$, $N(x,t) \doteq \langle n \rangle$, and $(\tilde{v}_x, \tilde{v}_y) = \hat{\boldsymbol{z}} \times \nabla\tilde{\varphi}$.

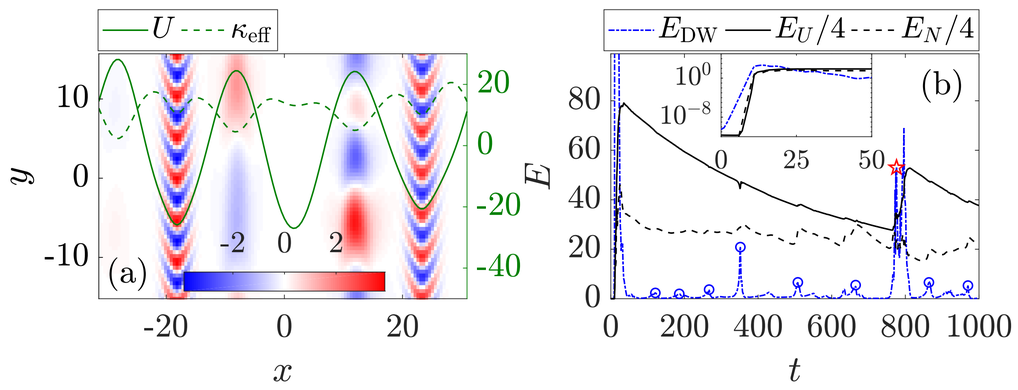

Figure 1: MHWE simulations with $\alpha = 5$, $\kappa = 12$, and $\hat{D} = 0.1\nabla^4$. (a) A snapshot showing $\tilde{w}$ (color), U (solid line), and $\kappa_{\rm eff} \doteq \kappa - \partial_x N$ (dashed line). (b) Evolution of DW and ZF energy, showing predator–prey oscillations.

Theory: tertiaty instability in the modified Hasegawa–Wakatani equations

- Assume a zonal state $U(x) = u\cos q_{\rm Z} x$ and $N(x) = 0$, and consider a perturbation $\tilde{w} = {\rm Re}[\psi(x) {\rm e}^{{\rm i}(p_y y - \omega t)}]$ on top. The linearized mHWE (1) leads to

$$\omega\psi = \hat{H}\psi, \quad \hat{H} = p_y[U + (\kappa + U'')\hat{\bar{p}}^{-2}] - {\rm i}\hat{D}, \quad \hat{\bar{p}}^2 \doteq \hat{p}_x^2 + p_y^2 + \frac{{\rm i}\alpha + p_y\kappa}{{\rm i}\alpha + {\rm i}\hat{D} + \omega - p_y U}, \quad \hat{p}_x \doteq -{\rm i}\frac{{\rm d}}{{\rm d}x}. \tag{3}$$

- Eigenmodes are found numerically, and we calculate the corresponding Wigner function $W(x,p_x) \doteq \int {\rm d}s\, {\rm e}^{-{\rm i}p_x s}\psi(x+s/2)\psi(x-s/2)$. It is found that W are localized at

$$x = x_n \doteq n\pi/q_{\rm Z}, \quad p_x = 0, \quad n = 0, \pm1, \pm2, \dots. \tag{4}$$

  They correspond to the extrema of U. Even n: trapped mode, odd n: runaway mode. [10, 11].
- Approximate U as $U \approx U_0 + \mathcal{C}x^2/2$, and Weyl-expand $\hat{H}$ as $\hat{H} \approx \mathcal{H} + \lambda_p \hat{p}_x^2 + \lambda_x x^2$, where the coefficients are given in Ref. [5]. This leads to an harmonic-oscillator equation:

$$-\lambda_p \psi'' + \lambda_x x^2 \psi = (\omega - \mathcal{H})\psi. \tag{5}$$

- Eigenmodes are given by Hermite polynomials H_m, where $m = 0, 1, ...$:

$$\psi_m = {\rm e}^{-\frac{x^2}{2\lambda}} H_m(x/\sqrt{\lambda}), \quad \omega_m = \mathcal{H} + (2m+1)\lambda_x\lambda. \tag{6}$$

- The two modes with $m = 0$ ($\mathcal{C} \gtrless 0$) are most unstable. The growth rates are:

$$\gamma_{\rm TI} \doteq {\rm Im}\,\omega_0 = \gamma_{\rm PI} + \Delta\gamma(\mathcal{C}), \quad \Delta\gamma = \gamma_{\rm PI}\mathcal{C}/\kappa + {\rm Im}(\lambda_x\lambda), \quad \gamma_{\rm PI} = p_y\kappa/\bar{p}_0^2 - {\rm i}D_0. \tag{7}$$

At $\mathcal{C} = 0$, $\gamma_{\rm TI}$ reduces to $\gamma_{\rm PI}$. Therefore, the TI is a primary instability modified by the ZF.

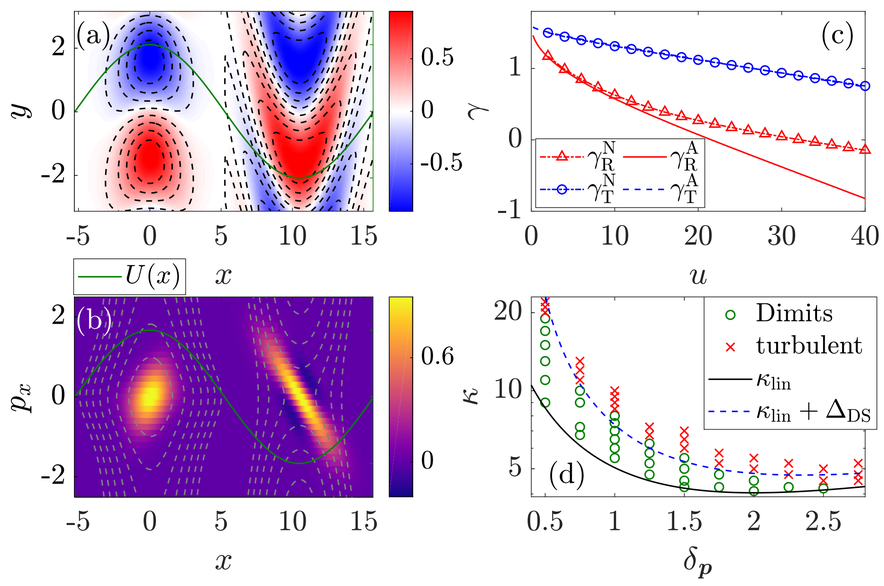

Figure 2: (a) Runaway and trapped mode structures: numerical (color) versus analytical (dashed contours) at $\alpha = 5$, $\kappa = 12$, $q_{\rm Z} = 0.3$, $u = 10$, and $p_y = 1$. (b) Same mode structures in phase space: Wigner functions (color) versus drifton trajectories (dashed contours). (c) Numerical and analytical growth rates. (d) Dimits shift in the limit of mTHE: simulation results (green circles and red crosses) versus analytic results (with $p_y = 1$ and $\varrho = 0.05$).

Overview of the main results [5, 6]

- We propose a very basic yet quantitative model of the TI and the Dimits shift.
- Models used: the modified Hasegawa–Wakatani equation (mHWE) [7], the modified Terry–Horton equation (mTHE) [8], and the ion-temperature-gradient (ITG) model [2].
- The TI can be described as quantum harmonic oscillators with complex frequencies.
- The TI threshold is shifted compared to the homogeneous turbulence. This shift corresponds to the Dimits shift in the mTHE.

Motivation: localized TI modes in electrostatic ITG turbulence

- We also observed similar localized ITG modes in GK simulations of a three-dimensional periodic box with zero magnetic shear.
- Box lengths: $L_x/\rho_{\rm i} = 10\pi$, $L_y/\rho_{\rm i} = 2\pi$, and $L_z/a = 20\pi$, where $\rho_i = v_i/\Omega_i$, v_i is the ion thermal velocity, Ω_i is the gyrofrequency, a is a reference length. Ions: $L_T/a = 0.5$, $L_n/a = 2.5$, and $\nu_{\rm ii} = 0.05 v_{\rm i}/a$. Electrons: $T_{\rm e} = T_{\rm i}$, adiabatic response except to the zonal mode, as usual.

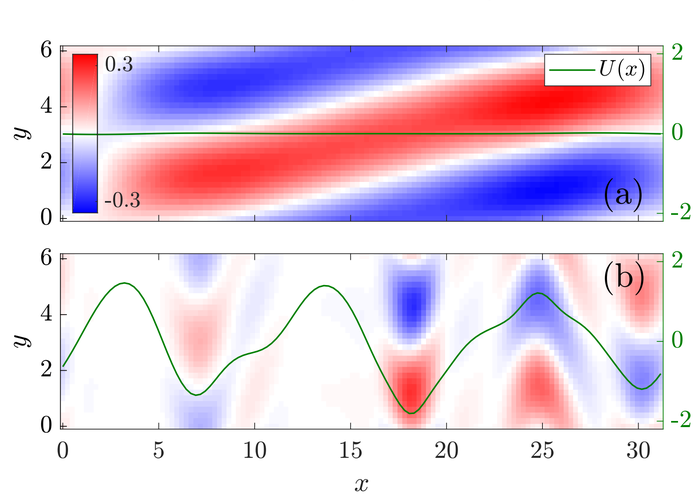

Figure 3: Gyrokinetic ITG simulation using the code GS2 [9]. (a) Linear stage, when the ITG mode grows exponentially. (b) Nonlinear stage, when the ZF is strong and the ITG modes are localized.

The TI threshold corresponds to the Dimits shift in the large-α limit

- In the large-α limit, electrons respond adiabatically ($N \approx 0$). The mHWE reduces to the mTHE:

$$(\partial_t + \hat{\boldsymbol{z}} \times \nabla\varphi \cdot \nabla) w = \kappa \partial_y \varphi - \hat{D} w, \quad \tilde{w} = (\nabla^2 - 1 + {\rm i}\hat{\delta})\tilde{\varphi}, \quad \langle w \rangle = \nabla^2 \langle \varphi \rangle \quad \delta_{\boldsymbol{p}} \doteq \kappa p_y^2/[\alpha(1+p_y^2)]. \tag{8}$$

- The growth rate can be found explicitly in this limit:

$$\gamma_{\rm TI} = {\rm Im}\left[\frac{p_y(\kappa + \mathcal{C})}{1 + p_y^2 - {\rm i}\delta_{\boldsymbol{p}}}\left(1 - \sqrt{\frac{\mathcal{C}}{2(\kappa + \mathcal{C})}}\right)\right] - D_0 = \gamma_{\rm PI} + \Delta\gamma(\mathcal{C}). \tag{9}$$

- The instability threshold is shifted compared with the primary-instability threshold:

$$\Delta_{\rm DS} = \kappa_{\rm c} - \kappa_{\rm lin}, \quad \kappa_{\rm c} = \frac{D_0}{p_y}\frac{(1+p_y^2)^2 + \delta_{\boldsymbol{p}}^2}{\delta_{\boldsymbol{p}} - (1+p_y^2)\sqrt{\varrho/2}}, \tag{10}$$

  where $\kappa_{\rm lin} \doteq \kappa_{\rm c}|_{\varrho=0}$ is the linear threshold of the primary instability and $\varrho \doteq \mathcal{C}/\kappa \approx {\rm const}$.
- The quantity $\Delta_{\rm DS}$ is the Dimits shift. At $\kappa > \kappa_{\rm c}$ the ZF is too weak to suppress the TI.

The same approach can be used to study the tertiary instability of ITG turbulence

- Two-dimensional gyrofluid model used in Ref. [2]:

$$\partial_t n + \hat{\boldsymbol{z}} \times \nabla\phi \cdot \nabla n + \hat{\boldsymbol{z}} \times \nabla(\tau\nabla^2\phi) \cdot \nabla T/2 = 0, \quad \partial_t T + \hat{\boldsymbol{z}} \times \nabla\phi \cdot \nabla T = 0, \tag{11}$$

  where $\tau = T_{\rm i}/T_{\rm e}$, ϕ is the gyroaveraged electrostatic potential, T is the guiding-center perpendicular temperature, and $n \doteq (1 - \tau\nabla^2)(\phi - \langle\phi\rangle) - \nabla^2(\phi + \tau T/2)$ is the guiding-center density.
- Zonal state and perturbations:

$$\phi = \phi_0(x) + \tilde{\phi}(x){\rm e}^{{\rm i}(p_y y - \omega t)}, \quad T = T_0(x) + \tilde{T}(x){\rm e}^{{\rm i}(p_y y - \omega t)}, \quad n_0 = -\phi_0'' - \tau T_0''/2. \tag{12}$$

  Then, $\tilde{n} = (1 + \tau\hat{p}^2 + \hat{p}^2)\tilde{\phi} + \tau\hat{p}^2\tilde{T}/2$, where $\hat{p}^2 \doteq -\nabla^2$.
- Define $U(x) \doteq \phi_0'$, $\bar{\omega}(x) \doteq \omega - p_y U$, and assume that $\eta \doteq T_0'$ is a positive constant. Then

$$\omega\tilde{n} = \hat{H}\tilde{n}, \quad \hat{H} = p_y U + p_y(U'' + \tau\eta\hat{p}^2/2 - p_y\tau\eta U''/2\bar{\omega})\hat{A}^{-1}, \quad \hat{A} = 1 + (1+\tau)\hat{p}^2 - p_y\eta\tau\bar{\omega}^{-1}\hat{p}^2/2.$$

- Also assume $U \approx U_0 + \mathcal{C}x^2/2$ and expand the Hamiltonian as $\hat{H} \approx \mathcal{H} + \lambda_p\hat{p}_x^2 + \lambda_x x^2$. One obtains real frequency: ${\rm Re}\,\omega \approx p_y U_0$, growth rate: ${\rm Im}\,\omega \sim p_y\sqrt{\tau\eta\mathcal{C}}$, mode width: $\Delta x \sim (\tau\eta/\mathcal{C})^{1/4}$.

The trapped TI mode can develop into an avalanche-like propagating structure (mHWE)

- Two types of predator–prey oscillations are observed and related to the TI.
- First type: the TI grows but is quickly suppressed by the modification of the zonal density.
- Second type: a trapped TI mode is not suppressed but develops into a propagating structure. This happens only when the ZF amplitude u is below a certain threshold $u_{\rm c}$.
- The corresponding critical shear $S_{\rm c} \doteq q_{\rm Z}u_{\rm c}$ scales linearly with $\gamma_{\rm TI}$.

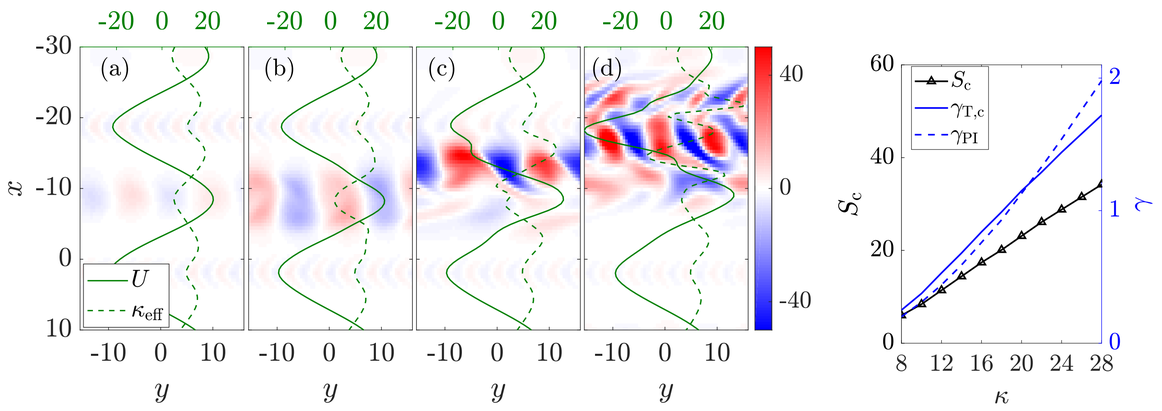

Figure 4: Left: Snapshots of a propagating structure corresponding to the red star in Fig. 1. Both the minimum and the maximum of U are amplified by this structure. Right: The critical shear $S_{\rm c}$.

Acknowledgment

This work was supported by the US DOE through Contract No. DE-AC02-09CH11466. This work made use of computational support by CoSeC, the Computational Science Centre for Research Communities, through CPP Plasma (EP/M022463/1) and HEC Plasma (EP/R029148/1).

References

[1] A. M. Dimits *et al.* Phys. Plasmas **7**, 969 (2000).

[2] B. N. Rogers, W. Dorland, and M. Kotschenreuther, Phys. Rev. Lett. **85**, 5336 (2000).

[3] S. Kobayashi and B. N. Rogers, Phys. Plasmas **19**, 012315 (2012).

[4] C.-B. Kim, B. Min, and C.-Y. An, Plasma Phys. Control. Fusion **61** 035002 (2019).

[5] H. Zhu, Y. Zhou, and I. Y. Dodin, Phys. Rev. Lett. **124**, 055002 (2020).

[6] H. Zhu, Y. Zhou, and I. Y. Dodin, J. Plasma Phys. **86**, 905860405 (2020).

[7] R. Numata, R. Ball, and R. L. Dewar, Phys. Plasmas **14**, 102312 (2007).

[8] D. A. St-Onge, J. Plasma Phys. **83**, 905830504 (2017).

[9] M. Barnes *el al.*, GS2 v8.0.2, https://doi.org/10.5281/zenodo.2645150.

[10] H. Zhu, Y. Zhou, D. E. Ruiz, and I. Y. Dodin, Phys. Rev. E **97**, 053210 (2018); H. Zhu, Y. Zhou, and I. Y. Dodin, Phys. Plasmas **25**, 072121 (2018); Phys. Plasmas **25**, 082121 (2018).

[11] D. E. Ruiz, J. B. Parker, E. L. Shi, and I. Y. Dodin, Phys. Plasmas **23**, 122304 (2016).